PAPER

Check for updates

A new G-triplex-based strategy for sensitivity enhancement of the detection of endonuclease activity and inhibition†

Congcong Gao, [ID] Baoquan Che and Hong Dai*

EcoRI is an important biomacromolecule in live cells and protects bacterial cells against foreign DNA. In this work, we developed a simple and convenient G-triplex (G3) (5′-TGGGAAGGGAGGGAATTCCCT-3′)-based colorimetric assay for the rapid and selective detection of EcoRI activity and inhibition. The sequence specifically responds to EcoRI in the presence of K^+ and hemin to form a G-triplex/hemin complex. Taking advantage of G-triplex, EcoRI activity was investigated under the optimized conditions. The absorption intensity ratio displayed a linear relationship against the concentration of EcoRI in the range 0 to 100 U mL^{-1}, and the detection limit was 5.7 U mL^{-1}. Furthermore, G3 showed good selectivity, and the ability to be used to screen for EcoRI inhibitors, indicating its potential in detection and analysis applications.

1. Introduction

Endonucleases play many significant roles in biological processes, with examples of these roles including DNA replication, DNA repair, DNA recombination, genotyping, and enzymatic amplification.[1–5] They can hydrolyze phosphodiester linkages with high specificity. In addition, endonucleases are also versatile targets in the development of drugs.[6–10] Inhibiting enzymes is one of the most important ways to control metabolic reactions and regulate biological processes.[11–13] Therefore, efficient enzyme inhibitors are often potential drug candidates for anticancer and antiparasite chemotherapy. So it is significant and desirable to develop approaches for detecting endonuclease activity and inhibition in molecular biology and drug development processes. Numerous analytical methods for endonuclease activity and inhibition have been established, with examples of these methods including polyacrylamide gel electrophoresis,[14] chromatography, enzyme-linked immunosorbent assays,[14–17] and fluorescence.[18–20] However, these approaches often are time consuming, laborious, and expensive, and yield results not amenable to being evaluated using the naked eye.

G-Quadruplex (G4), which comprises four tandem G-tracts, has been widely used in oncology,[21] recognition probes,[22,23]
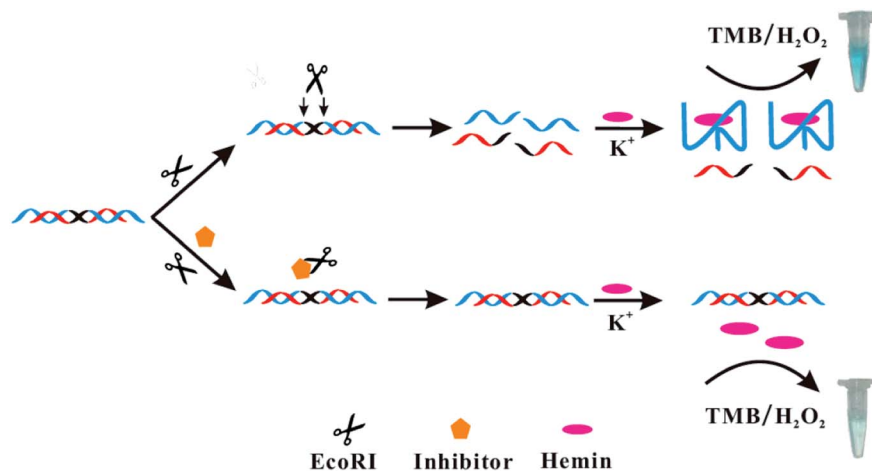
biosensors,[24] and nanotechnology[25,26] due to the diversity of its forms and flexibility of its conformational switch. G-quadruplex has certain limitations in high background signal and the hybridized section is not easily unwound after cleaved by EcoRI.[27,28] For example, undesired intermolecular G-quadruplex structures may form, and these structures may show high background interference. Recent reports found that G-triplex (G3) is a promising replacement for G-quadruplex. Compared to G-quadruplex, G-triplex generally needs fewer G-tracts and results in lower background interference, making it more suitable for use in biosensing development.[29–32] Gao *et al.* demonstrated a G-triplex switch that can be triggered by changing the pH, and exhibiting good on-off reversibility upon reversing the change in pH.[33] Zhou *et al.* developed a stable G-triplex-based light-up fluorescent probe that was successfully applied for miRNA detection.[34] Wen *et al.* devised a dual-functional peptide-PNA (peptide nucleic acid) conjugate that was shown to impact the tracking activity of motor proteins on DNA with superior selectivity and potency.[35]

In this work, the EcoRI restriction endonuclease was chosen as a model enzyme. We developed a new G-triplex-based colorimetric assay for the rapid, sensitive and selective detection of EcoRI activity and inhibition. The working principle is shown in Scheme 1. We rationally designed a dsDNA substrate. This substrate was constructed from the self-hybridization of two identical ssDNA sequences. The ssDNA contained three functionally distinct regions: an enzyme recognition region (black in Scheme 1), G-triplex sequence region (blue), and blocking region (red). Without EcoRI, the G-triplex was blocked by the corresponding blocking region in the dsDNA substrate and no G-triplex structure was formed. The color of a chromogenic TMB/H_2O_2 liquid to which K^+ and hemin were added

Beijing Institute for Drug Control, MNPA Key Laboratory for Quality Evaluation of Traditional Chinese Medicine (Traditional Chinese Medicine), MNPA Key Laboratory for Research and Evaluation of Generic Drugs, Beijing Key Laboratory of Analysis and Evaluation on Chinese Medicine, Beijing 102206, China. E-mail: gcc1125@163. com

Scheme 1 Illustration of the colorimetric assay used for studying EcoRI activity and inhibition based on G-triplex.

became pale blue. However, in the presence of EcoRI, the dsDNA substrate cleaved into two parts. The thermostability of the cleaved dsDNA was markedly decreased and the cleaved dsDNA was separated into several ssDNA parts. Since the blocked G-triplex sequence was released, addition of K^+ and hemin led to formation of a G-triplex/hemin complex. The color of the chromogenic TMB/H_2O_2 liquid to which this complex was added became obviously blue, attributed to the enhanced catalytic ability of the complex. Thus, the EcoRI activity could be assessed by simply inspecting the color of the reaction solution.

2. Experimental section

2.1. Materials and instruments

The oligonucleotides used in this work were synthesized using TaKaRa Clontech to have the sequences

G3, 5′-TGGGAAGGGAGGGAATTCCCT-3′, G4a, 5′-GGGTAGGGCGGGTTGGGAATTCCCA-3′, and

G4b, 5′-GGGTAGGGCGGGTTGGGAATTCCCACCCG-3′.

EcoRI endonuclease (Lot: 10092924), BamHI endonuclease (Lot: 10086715), T4 polynucleotide kinase (Lot: 10088982), endonuclease IV (Lot: 10088353), and Nt.BstNBI (Lot: 10068267) were obtained from New England Biolabs Inc. Hemin ($C_{34}H_{32}$-ClN_4O_4Fe, Lot: H2028150) was purchased from Shanghai Aladdin Biochemical Technology Co., Ltd. 5-Fluorouracil (Lot: GC22BA0009) was obtained from Sangon Biotechnology Inc. (Shanghai, China). 3,3′,5,5′-Tetramethylbenzidine ($C_{16}H_{20}N_2$, TMB, Lot: SLCF1838) was obtained from Sigma-Aldrich. Tris–HCl buffer (1 M, pH = 7.4, Lot: 20200708) was purchased from Solarbio. Other reagents were of analytical grade and obtained from standard reagent suppliers. All solutions were prepared using Milli-Q water with a resistivity of 18.2 MΩ cm^{-1}. Absorption spectra were recorded using a Purkinje TU-1901 spectrophotometer.

Buffer A used in this work was composed of 50 mM NaCl and 20 mM Tris–HCl buffer, pH 7.4. DNA for the reaction was prepared by combining 10 μL of oligonucleotides (100 μM) with 90 μL of buffer A, annealing the resulting solution at 90 °C for 10 minutes and then cooling it to room temperature, and finally storing the cooled solution at 4 °C.

2.2. Practicability

G3 was designed to assess the feasibility of the protocol. After being subjected to annealing, 10 μL of DNA was added into a 100 μL system containing 10 μL of NE buffer (10×, 100 mM Tris–HCl, 50 mM NaCl, 10 mM MgCl$_2$, 0.025% Triton X-100, pH 7.5), 1 μL of EcoRI (20 000 U mL^{-1}) and 79 μL of ultra-pure water. The reaction mixture was subjected to gentle shaking at 37 °C for 3 h, and then 50 μL of hemin (1 μM) and 50 μL of K^+ (100 mM) were introduced into the mixture. The resulting mixture was incubated at 25 °C for 1 h. Then, 50 μL of TMB with 150 μL ultra-pure water were added into the incubated mixture and then together mixed for 20 min. All control samples were the same as the above samples but without EcoRI. Absorption spectra at 650 nm were recorded.

2.3. Optimization of reaction conditions

To acquire the best analytical performances, a series of experimental parameters including the amounts of DNA, hemin and TMB, and the incubation time of EcoRI were examined and optimized.

2.4. Investigation of selectivity

The anti-interference capability of the proposed method was investigated. Here, various enzymes were tested, including EcoRI endonuclease, T4 polynucleotide kinase, BamHI endonuclease, endonuclease IV, and Nt.BstNBI. The concentration of each of these enzymes was 100 U mL^{-1}.

2.5. Assay of EcoRI activity and inhibition

Under the above optimum conditions, various concentrations of EcoRI (from 0 to 100 U mL^{-1}) and the inhibitor 5-fluorouracil (from 0 to 0.3 mM) were tested.
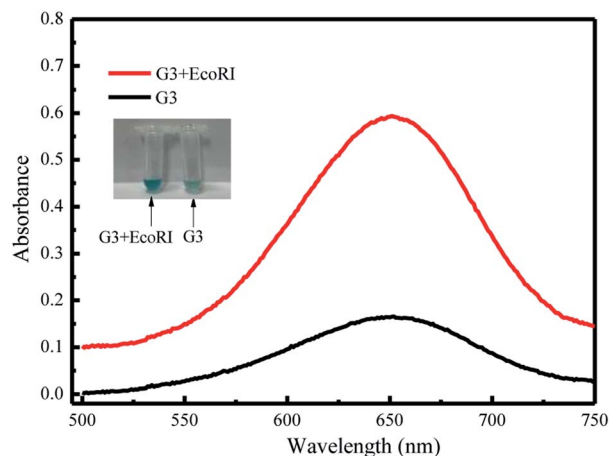
Fig. 1 Absorption spectra of G3 (0.25 μM) in the absence and presence of EcoRI (200 U mL^{-1}). Inset: photograph of colorimetric tubes of the above two solutions.

3. Results and discussion

3.1. Practicability

To demonstrate the feasibility of the proposed method, the response of G3 to EcoRI was first evaluated spectroscopically. In the absence of EcoRI, G3 displayed weak absorption of light centered at a wavelength of 650 nm. After addition of EcoRI, the absorption at 650 nm was significantly enhanced (Fig. 1). The change in the spectrum was a result of the formation of the G-triplex/hemin complex, as illustrated in Scheme 1. A CD spectroscopy analysis was also carried out (Fig. S1†); in the presence of K$^+$, the reaction products were indicated from the CD results to be folded into a G-triplex form, and the structure of G-triplex was also stable when it was bound to hemin.

3.2. Optimization of experimental conditions

Next, several factors were optimized including the G3 concentration (0.25 to 5.0 μM), reaction time with EcoRI (30 to 240 minutes), concentration of hemin (0.125 to 1.5 μM) and that of TMB (40 to 80 μL). The signal-to-noise (S/N) ratio A/A_0 was used

to assess the impacts of various parameters, where A and A_0 are the absorption intensities of G3 with and without EcoRI, respectively. The performances including the G3 concentration (0.25 to 5.0 μM), the reaction time of EcoRI (30 to 240 min), concentration of hemin (0.125 to 1.5 μM) and TMB (40 to 80 μL) were investigated when the concentration of EcoRI was 200 U mL^{-1}. The optimal concentration of DNA was 2.5 μM (Fig. S2†), and the reaction time with EcoRI was made to be 3 hours to ensure a complete response (Fig. S3†). Also, the optimized concentration of hemin was 0.5 μM (Fig. S4†), and a TMB volume of 50 μL was considered to be appropriate (Fig. S5†).

3.3. Evaluation of endonuclease activity

Under the optimal conditions, the reaction kinetics was investigated by performing absorption spectroscopy. Upon gradually increasing the concentration of EcoRI, the absorption intensity centered at 650 nm increased (Fig. 2A), and the color changed from light blue to dark. The A/A_0 values for various EcoRI concentrations (0 U mL^{-1}, 10 U mL^{-1}, 20 U mL^{-1}, 40 U mL^{-1}, 60
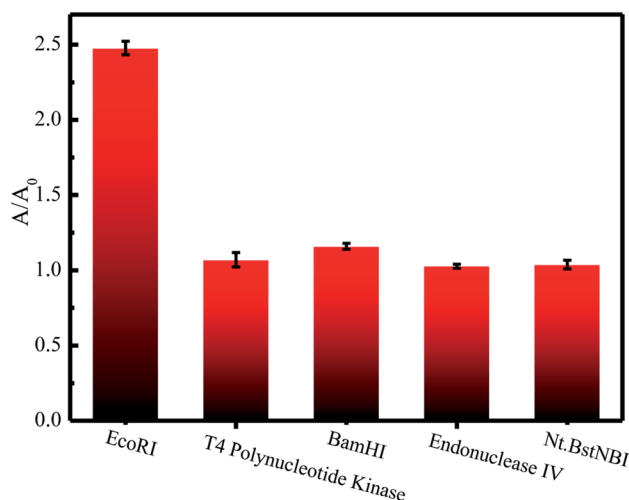

Fig. 3 Responses of G3 (2.5 μM) to the presence of various enzymes (100 U mL^{-1}) including EcoRI endonuclease, T4 polynucleotide kinase, BamHI endonuclease, endonuclease IV, and Nt.BstNBI.
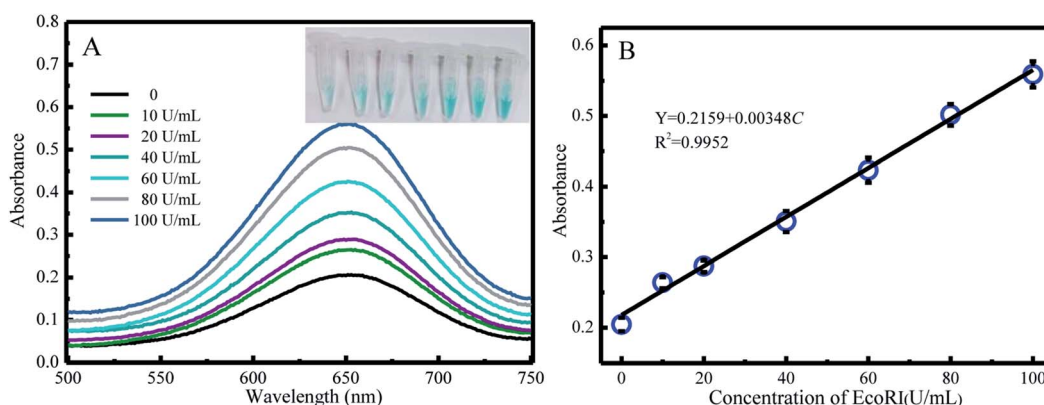

Fig. 2 (A) Absorption spectra (main figure) and photograph (inset) of various solutions of different concentrations of EcoRI (0–100 U mL^{-1}). (B) Plot of peak absorbance intensity versus concentration of EcoRI. A linear relationship was observed.

© 2021 The Author(s). Published by the Royal Society of Chemistry

U mL^{-1}, 80 U mL^{-1}, and 100 U mL^{-1}) were determined and are shown in Fig. 2B. The limit of detection (LOD) value was calculated to be 5.7 U mL^{-1} on the basis of S/N = 3.

3.4. Selectivity of G3

The specificity of G3 toward EcoRI was evaluated. G3 was incubated with various enzymes including EcoRI endonuclease, T4 polynucleotide kinase, BamHI endonuclease, endonuclease IV, and Nt.BstNBI. Only EcoRI induced a dramatic absorption enhancement, while others triggered limited changes (Fig. 3). This set of results demonstrated that G3 can respond to EcoRI with high specificity.

3.5. EcoRI endonuclease inhibition assay

The inhibitors of endonucleases are potential candidates for many antimicrobial and antiviral drugs.[11] Therefore, it is essential to develop methods for assaying endonuclease inhibition. According to previous reports, 5-fluorouracil has been used extensively in the treatment of solid tumors for many years,[36] and is an inhibitor of EcoRI endonuclease.[37–39] Hence, the inhibitory effect of 5-fluorouracil was investigated in the current work. As is shown in Fig. 4, the activity of EcoRI endonuclease decreased as the concentration of 5-fluorouracil was increased, illustrating that G3 can be used to screen inhibitors of endonuclease.

3.6. Traditional G-quadruplex strategies

To prove that our proposed G-triplex-based strategy is better than the traditional G-quadruplex strategy in sensitivity, a comparison between the traditional G-quadruplex method and the G-triplex method was made. As shown in Fig. 5, applications of the two G-quadruplex-based designs only caused minor absorption changes, far less than that caused by application of the G-triplex-based design. Application of the G4a substrate may have induced the generation of a high background (noise) caused by the unhybridized G3 section, hence
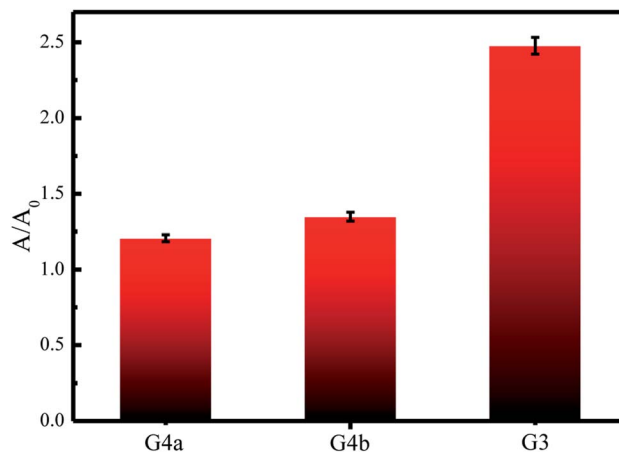

Fig. 5 Responses of G4a, G4b and G3 (2.5 μM) to EcoRI under the same conditions.

decreasing the signal-to-background ratio. Application of the G4b substrate may not have induced the generation of a background as high as that induced by G4a—but the hybridized section was not easily unwound after being cleaved by EcoRI enzyme and hindered the formation of G-quadruplex, with this hindrance also decreasing the signal-to-background ratio. However, application of the G3 substrate apparently was able to reduce the background and the applied G3 was apparently easily unwound as a result of EcoRI enzyme cleavage. Compare with G-quadruplex, G-triplex contains only three G-tracts,[34,40–43] making it easier to form G-triplex/hemin complex after reacting with the target and reduce the background in the absence of target. Therefore, use of the shorter G-rich G-triplex was deemed to be preferred to the use of the traditional G-quadruplex strategy for sensitively detecting EcoRI activity and inhibition.

4. Conclusions

In summary, a simple and colorimetric strategy based on a new G-triplex for the determination of EcoRI activity and inhibition levels was established. The approach exhibited high sensitivity and specificity toward EcoRI endonuclease. By comparison, G-triplex showed less complementary hybridization of G-rich sequences than did G-quadruplex, which resulted in obvious signal changes. The G-triplex strategies showed easy responses and rapid reactions, indicating their great potential in being applied to biochemical detection and analysis.

Conflicts of interest

There are no conflicts to declare.

References

1 N. D. F. Grindley, K. L. Whiteson and P. A. Rice, Mechanisms of site-specific recombination, *Annu. Rev. Biochem.*, 2006, **75**(1), 567–605.
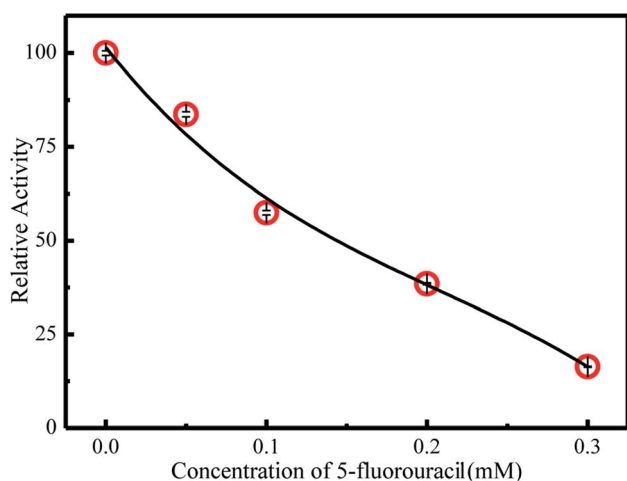
Fig. 4 Plot of the inhibitory effect of 5-fluorouracil (0, 0.05 μM, 0.1 μM, 0.2 μM, 0.3 μM) on the activity of EcoRI (100 U mL^{-1}).

2 M. R. Lieber, The FEN-1 family of structure-specific nucleases in eukaryotic DNA replication, recombination and repair, *BioEssays*, 1997, **19**(3), 233–240.

3 T. M. Marti and O. Fleck, DNA repair nucleases, *Cell. Mol. Life Sci.*, 2004, **61**(3), 336–354.

4 F. Sang, *et al.*, A hairpin-type DNA probe for direct colorimetric detection of endonuclease activity and inhibition based on the deaggregation of gold nanoparticles, *Microchim. Acta*, 2019, **186**(2), 1–7.

5 X. Xu, M. S. Han and C. A. Mirkin, A Gold-Nanoparticle-Based Real-Time Colorimetric Screening Method for Endonuclease Activity and Inhibition, *Angew. Chem.*, 2007, **46**(19), 3468–3470.

6 B. M. Baughman, *et al.*, Identification of Influenza Endonuclease Inhibitors Using a Novel Fluorescence Polarization Assay, *ACS Chem. Biol.*, 2012, **7**(3), 526–534.

7 E. De Clercq, Antiviral agents active against influenza A viruses, *Nat. Rev. Drug Discovery*, 2006, **5**(12), 1015–1025.

8 S. Y. Choi, *et al.*, Antimicrobial susceptibility and strain prevalence of Korean vaginal Lactobacillus spp, *Anaerobe*, 2003, **9**(6), 277–280.

9 D. M. Heithoff, *et al.*, An Essential Role for DNA Adenine Methylation in Bacterial Virulence, *Science*, 1999, **284**(5416), 967–970.

10 K. D. Robertson and A. P. Wolffe, DNA methylation in health and disease, *Nat. Rev. Genet.*, 2000, **1**(1), 11–19.

11 A. K. Ghosh and H. L. Osswald, BACE1 (β-secretase) inhibitors for the treatment of Alzheimer's disease, *Chem. Soc. Rev.*, 2014, **43**(19), 6765–6813.

12 S. P. Gupta, QSAR studies on enzyme inhibitors, *Chem. Rev.*, 1987, **87**(5), 1183–1253.

13 J. Borch and P. Roepstorff, Screening for Enzyme Inhibitors by Surface Plasmon Resonance Combined with Mass Spectrometry, *Anal. Chem.*, 2004, **76**(18), 5243–5248.

14 L. A. VanderVeen, *et al.*, Differential DNA Recognition and Cleavage by EcoRI Dependent on the Dynamic Equilibrium between the Two Forms of the Malondialdehyde−Deoxyguanosine Adduct, *Biochemistry*, 2005, **44**(13), 5024–5033.

15 G. Song, *et al.*, A Simple, Universal Colorimetric Assay for Endonuclease/Methyltransferase Activity and Inhibition Based on an Enzyme-Responsive Nanoparticle System, *ACS Nano*, 2009, **3**(5), 1183–1189.

16 D. J. Wright, W. E. Jack and P. Modrich, The Kinetic Mechanism of EcoRI Endonuclease*, *J. Biol. Chem.*, 1999, **274**(45), 31896–31902.

17 A. Jeltsch, *et al.*, A Fast and Accurate Enzyme-Linked Immunosorbent Assay for the Determination of the DNA Cleavage Activity of Restriction Endonucleases, *Anal. Biochem.*, 1993, **213**(2), 234–240.

18 J. Deng, *et al.*, Sensitive detection of endonuclease activity and inhibition using gold nanorods, *Biosens. Bioelectron.*, 2012, **34**(1), 144–150.

19 Y. Huang, *et al.*, Intermolecular and Intramolecular Quencher Based Quantum Dot Nanoprobes for Multiplexed Detection of Endonuclease Activity and Inhibition, *Anal. Chem.*, 2011, **83**(23), 8913–8918.

20 X.-Q. Jiang, *et al.*, DNA-hosted Hoechst dyes: application for label-free fluorescent monitoring of endonuclease activity, *Analyst*, 2014, **139**(22), 5682–5685.

21 H. Han and L. H. Hurley, G-quadruplex DNA: a potential target for anti-cancer drug design, *Trends Pharmacol. Sci.*, 2000, **21**(4), 136–142.

22 B. Jin, *et al.*, Fluorescence Light-Up Probe for Parallel G-Quadruplexes, *Anal. Chem.*, 2014, **86**(1), 943–952.

23 B. Jin, *et al.*, Dicyanomethylene-Functionalized Squaraine as a Highly Selective Probe for Parallel G-Quadruplexes, *Anal. Chem.*, 2014, **86**(14), 7063–7070.

24 S. Shimron, *et al.*, Amplified Detection of DNA through the Enzyme-Free Autonomous Assembly of Hemin/G-Quadruplex DNAzyme Nanowires, *Anal. Chem.*, 2012, **84**(2), 1042–1048.

25 S. Modi, *et al.*, A DNA nanomachine that maps spatial and temporal pH changes inside living cells, *Nat. Nanotechnol.*, 2009, **4**(5), 325–330.

26 G. I. Livshits, *et al.*, Long-range charge transport in single G-quadruplex DNA molecules, *Nat. Nanotechnol.*, 2014, **9**(12), 1040–1046.

27 S. Wang, *et al.*, The G-triplex DNA could function as a new variety of DNA peroxidase, *Chem. Commun.*, 2013, **49**(72), 7920–7922.

28 L.-L. Zhao, *et al.*, The Exploration of a New Stable G-Triplex DNA and Its Novel Function in Electrochemical Biosensing, *Anal. Chem.*, 2019, **91**(16), 10731–10737.

29 D. Koirala, *et al.*, Intramolecular folding in three tandem guanine repeats of human telomeric DNA, *Chem. Commun.*, 2012, **48**(14), 2006–2008.

30 V. Limongelli, *et al.*, The G-Triplex DNA, *Angew. Chem.*, 2013, **52**(8), 2269–2273.

31 W. Li, *et al.*, Direct Measurement of Sequential Folding Pathway and Energy Landscape of Human Telomeric G-quadruplex Structures, *J. Am. Chem. Soc.*, 2013, **135**(17), 6423–6426.

32 A. Rajendran, *et al.*, Small molecule binding to a G-hairpin and a G-triplex: A new insight into anticancer drug design targeting G-rich regions, *Chem. Commun.*, 2015, **51**(44), 9181–9184.

33 H. Gao, *et al.*, A pH-triggered G-triplex switch with K($^+$) tolerance, *Chem. Commun.*, 2020, **56**(53), 7349–7352.

34 H. Zhou, *et al.*, Stable and Label-Free Fluorescent Probe Based on G-triplex DNA and Thioflavin T, *Anal. Chem.*, 2018, **90**(5), 3220–3226.

35 C.-j. Wen, *et al.*, Targeting nucleic acids with a G-triplex-to-G-quadruplex transformation and stabilization using a peptide-PNA G-tract conjugate, *Chem. Commun.*, 2020, **56**(48), 6567–6657.

36 A. T. Hulme, S. L. Price and D. A. Tocher, A New Polymorph of 5-Fluorouracil Found Following Computational Crystal Structure Predictions, *J. Am. Chem. Soc.*, 2005, **127**(4), 1116–1117.

37 D. K. Jangir, *et al.*, FTIR and circular dichroism spectroscopic study of interaction of 5-fluorouracil with DNA, *J. Photochem. Photobiol., B*, 2011, **105**(2), 143–148.

38 Y. Huang, *et al.*, Multiplex Detection of Endonucleases by Using a Multicolor Gold Nanobeacon, *Chem.–Eur. J.*, 2011, **17**(26), 7313–7319.

39 L. Ma, *et al.*, Microarray-based fluorescence assay of endonuclease functionality and inhibition, *Analyst*, 2013, **138**(4), 1048–1052.

40 J. Gao, *et al.*, Comparative evaluation and design of a G-triplex/thioflavin T-based molecular beacon, *Analyst*, 2021, **146**(8), 2567–2573.

41 J. H. Yum, S. Park and H. Sugiyama, G-quadruplexes as versatile scaffolds for catalysis, *Org. Biomol. Chem.*, 2019, **17**(44), 9547–9561.

42 Z. Wu, *et al.*, G-triplex based molecular beacon with duplex-specific nuclease amplification for the specific detection of microRNA, *Analyst*, 2019, **144**(17), 5201–5206.

43 R. Li, *et al.*, Sensitive colorimetric determination of microRNA let-7a through rolling circle amplification and a peroxidase-mimicking system composed of trimeric G-triplex and hemin DNAzyme, *Microchim. Acta*, 2020, **187**(2), 139.